

The Role of Plasma Chemistry Parameters in Cancer Therapy by Plasma Jet

Elahesadat Torabibashkani¹, Kiomars Yasserian^{*1}, Majid Borghei¹, Hamideh Mahmoodzadeh Hosseini², Amir Hossein Sari³

¹*Department of Physics, Karaj Branch, Islamic Azad University, Karaj, Iran*

²*Applied Microbiology Research Center, Biomedicine Technologies Institute, Baqiyatallah University of Medical Sciences, Tehran, Iran*

³*Plasma Physics Research Center, Sciences and Research Branch, Islamic Azad University, Tehran, Iran*

(Received 22 Feb. 2024; Final revised received 05 May 2024)

Abstract

Atmospheric pressure plasma jet (APPJ) is one of the efficient methods to treat cancer cells. It is known that by setting the plasma parameters such as plasma density and temperature by variation of applied voltage on the plasma jet device, the plasma can induce apoptosis in cancer cells and reduce tumor growth without significant influence on healthy cells. To gain deeper insights into the influence of voltage variations and the type of working gas, a simulation of APPJ was conducted using Comsol Multiphysics software. To complete the simulation, various chemical features were considered, such as surface reactions, elastic collision cross-sections, and ionization and excitation cross-sections, which depend on the plasma energy. The dependence of the plasma temperature and density on the applied voltage and types of working gas was also investigated. It was found that higher voltage results in an increase in the plasma temperature and electron density. As the input voltage increased, both the plasma pressure and its spatial nonuniformity within the plasma tube showed a noticeable rise. In addition, the overall values of the electric potential for gas working of He is higher than the argon gas.

Keywords: Plasma Chemistry Parameters, Atmospheric Pressure Plasma Jet, Plasma Cancer Therapy, Helium Plasma, Argon Plasma.

^{*}**Corresponding author:** *Kiomars Yasserian, Department of Physics, Karaj Branch, Islamic Azad University, Karaj, Iran, Email: Kiomars.yasserian@kiau.ac.ir.*

Introduction

Cold atmospheric plasma (CAP) is a novel and promising modality for anticancer treatment that can overcome drug resistance in cancer [1-3]. The selective operation of CAP in cancer therapy (as an auxiliary treatment), specifically targets cancer cells while sparing healthy cells [4,5]. This unique ability of plasma therapy is a result of the potential of CAP to create an environment rich in reactive species, neutral particles, electromagnetic fields, and UV radiation. This ability enables various recent biomedical applications, including cancer therapy. [6]

There are various types of cold plasma, including dielectric barrier discharge (DBD), corona discharge, plasma needles, and plasma jets [7-8]. However, recent studies on the application of CAP cancer therapy have primarily focused on DBDs and plasma jets [9-10].

Many researchers [11] and the references have studied the effects of different controlling parameters, such as applied voltage and gas flow rate on plasma jet characteristics, such as electron density, electron temperature, and electric potential therein. The focus of the investigations is on the mechanism of plasma formation and the interaction of plasma with tissues to optimize the treatment conditions for biomedical applications. In the previous study an atmospheric pressure plasma jet device has been designed and fabricated to interact with the colorectal cancer cells [12]. In addition, For example, Ref. [13] studied the Laminar plasma plumes, which were characterized by a smooth and steady flow of plasma and it provided a controlled and uniform distribution of reactive species, such as reactive oxygen species (ROS), which were known to induce cell death in cancer cells. The laminar plumes can be advantageous in delivering a consistent and targeted treatment to the tumor site, minimizing damage to the healthy tissues surrounding the tumor.

Several studies have used Comsol software to simulate plasma jets and analyze electron density and temperature variations. Y. Amini et al. [14] simulated a plasma jet and investigated the effects of applied voltage and gas flow rate on CAP operation.

The applications of CAP depend on plasma characteristics such as the applied voltage; therefore, it is necessary to obtain optimized conditions [15]. Ref. [16] showed that the sinusoidal initiation voltage of the plasma jet should be optimized to maximize the effectiveness of CAP treatment on various cancer cell lines. It was shown that the optimal discharge voltage amplitude varied between 3 kV and 5 kV, with a frequency range of 13–50 kHz.

It is to be noted here that secondary electrons have a significant effect on the plasma formation and temporal evolution of the plasma plume. The secondary electron emission at the walls is comparable to electron production by ionization. The coefficient of secondary electron emission in the wall region affects the stationary distribution of the plasma parameters and electric field [17-19].

The interaction between the atmospheric pressure plasma jet and cells and tissue depends on the chemical components of the plasma. These components can induce opposite influences: a killing effect or a healing effect. Furthermore, it is well known that for a narrow range of plasma chemistry parameters, normal cells (healthy) are less sensitive to the killing effect of the atmospheric pressure plasma jet. This latter effect is known as the "selective behavior of the plasma," which enables the plasma to have fewer side effects in cancer therapy compared to other auxiliary medical treatments. Therefore, one of the focuses in cancer therapy using the APPJ is obtaining the optimal operational conditions to interact with cancer and healthy cells. In other words, the mentioned features of plasma cancer therapy relate to plasma chemistry.

In addition, there is a logical relationship between the reactive oxygen/nitrogen species (RONS) produced in the plasma and the selectivity features of the plasma in cancer therapy. The rate of produced reactive oxygen/nitrogen species (RONS) depends on the pattern of plasma parameters in the jet and the dynamic behavior of the plasma plume, particularly pressure, density, particle flux, and temperature. Therefore, our study focuses on the temporal behavior of two-dimensional plasma parameters for different gas types, applied voltages, and passing times to obtain the optimal conditions for cancer therapy as a possible auxiliary treatment. In our previous study [12], we experimentally obtained the optimum operational conditions for APPJ in cancer therapy, considering both direct and indirect interactions with healthy and cancer cells. Here, we simulate the APPJ using the aforementioned optimal parameters.

In this study, we modeled a two-dimensional atmospheric pressure plasma jet using Comsol Multiphysics software to investigate the temporal evolution of electron density and temperature distributions as a function of parameters such as applied voltage. Many researchers have investigated plasma formation in the plasma jet without considering the secondary electrons emission at the wall. The choice of electrode type can influence the quantity of secondary electrons generated. Altering the electrode type can result in an increase or decrease in the number of secondary electrons. Therefore, we have considered secondary electrons in our model. The paper has been organized as follows: Following the introduction, the model equations, including the boundary conditions are presented in Section 2. . In Sec. 3, numerical solutions of the model equations and their conclusions are explained. The findings of the study are succinctly presented in Section 4.

Experimental

To investigate the interaction of atmospheric pressure plasma with cells, a plasma jet has been designed and fabricated, with details of its size and geometrical configuration reported in Ref.18.

Figure 1 illustrates the two-dimensional geometry of the plasma jet. The device consists of a central pin electrode and a ring electrode made of copper, separated by a distance of 15 mm. A silica tube surrounds the pin electrode. The pin electrode is connected to a high-voltage source, and the ring electrode is grounded. In our previous study, a CAP was designed and developed to investigate the influence of cold plasma on cancer and non-cancer cells. In that investigation, the voltage was set at 2 and 5 kV, and the gas flow rate was maintained at 5 L/min. In this work, we are going to investigate the impact of varying applied voltage on plasma formation in the plasma jet device. It is crucial to assess and optimize several key factors, including voltage, frequency, and gas flow rate, to enhance the performance of the device.

In the present research, we specifically set the frequency to 35 (KHz) and investigated the effect of changing the plasma jet voltage on the flame properties of the plasma jet. Helium was used as the working gas at a flow rate of 5 L/min. The device operated at an applied voltage of 5 kV and a frequency of 35 kHz. The initial electron density was 10^6 m^{-3} at pressure of 1 atm. and a temperature of 300 K.

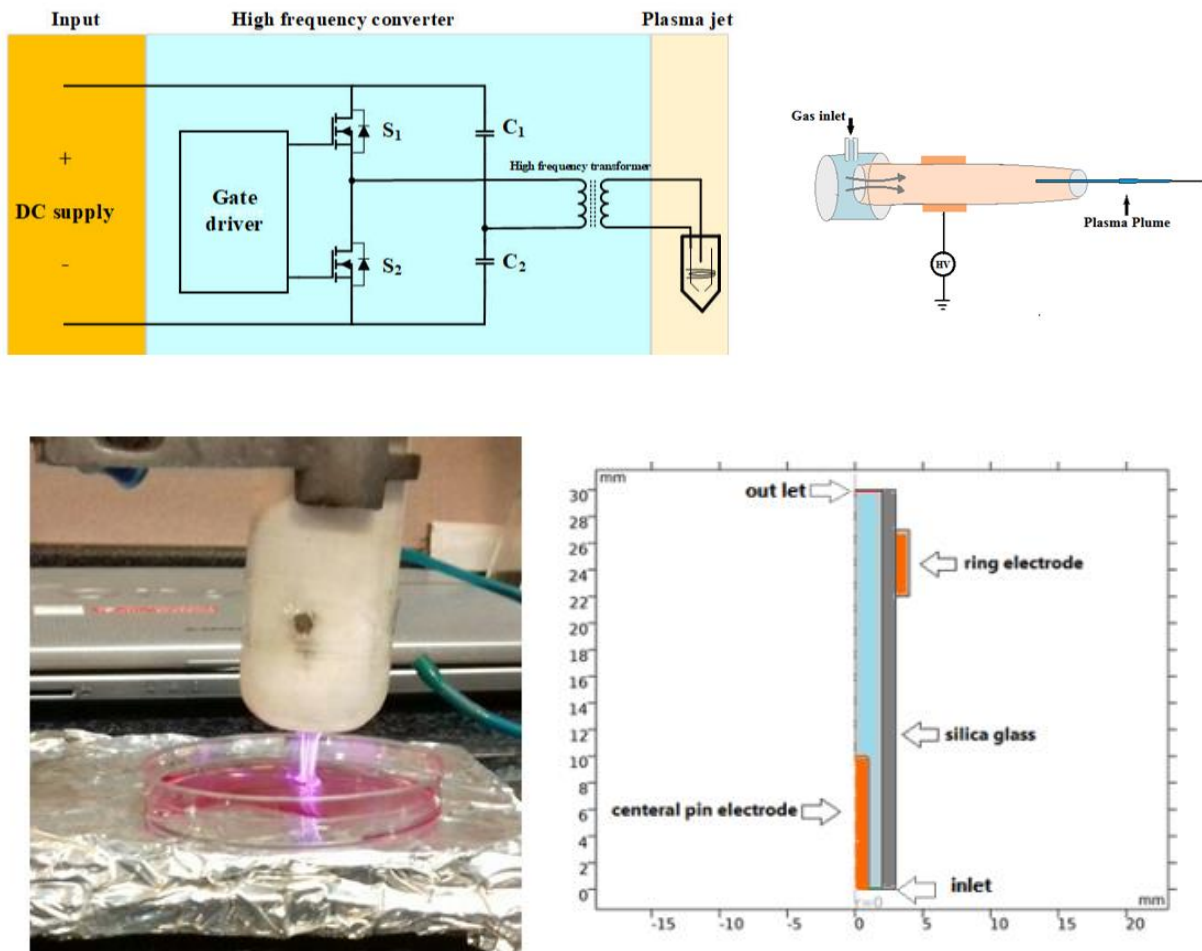


Figure 1. The Fabricated plasma jet and the-dimensional simulation region.

The fluid model, which includes the continuity and momentum transfer equations for ions, was used to simulate the atmospheric pressure plasma jet. The finite element method was employed to solve the set of fluid model using the COMSOL software [20].

$$\frac{\partial n_e}{\partial t} + \nabla \cdot \Gamma_e = R_e - (u \cdot \nabla) n_e \quad (1)$$

$$\Gamma_e = -(\mu_e \cdot E) n_e - D_e \cdot \nabla n_e \quad (2)$$

Where n_e denotes the electron density, D_e represents the electron diffusion coefficient, Γ_e signifies the electron flux vector, u and R_e is the average velocity of the particle fluid and electron production rate respectively.

In general, the energy of the electron flux is composed of two parts: the energy that the particles receive from the field and the energy that the particles receive from the reaction. The term $E \cdot \Gamma_e$ specifically expresses the energy that electrons receive from the electric field [21,22].

$$\frac{\partial n_e}{\partial t} + \nabla \cdot \Gamma_e + E \cdot \Gamma_e = R_e - (u \cdot \nabla) n_e \quad (3)$$

Because of their random movements, electrons collide with the walls, where they are absorbed and subsequently vanished. In addition, electrons are generated through secondary emissions. This continuous cycle of electron creation and destruction establishes the boundary conditions for the electron flux [23].

$$-n\Gamma_e = \frac{1}{2} \varepsilon_e n_e - \sum \varepsilon_p (n\Gamma_e) \quad (4)$$

$$-n\Gamma_e = \frac{5}{6} \varepsilon_e n_e - \sum \varepsilon_p \gamma_p (n\Gamma_e) \quad (5)$$

where ε_e , γ_p and ε_p are the collision frequency, the secondary diffusion coefficient and average energy of the secondary electrons respectively. It is assumed that the electric potential at the outer boundary is zero. Figure 2 shows the triangular meshing of the pin electrode, which was created using the finite element method (FEA). This meshing enables us to accurately capture the separation of the space charge in the boundary layers within the plasma volume.

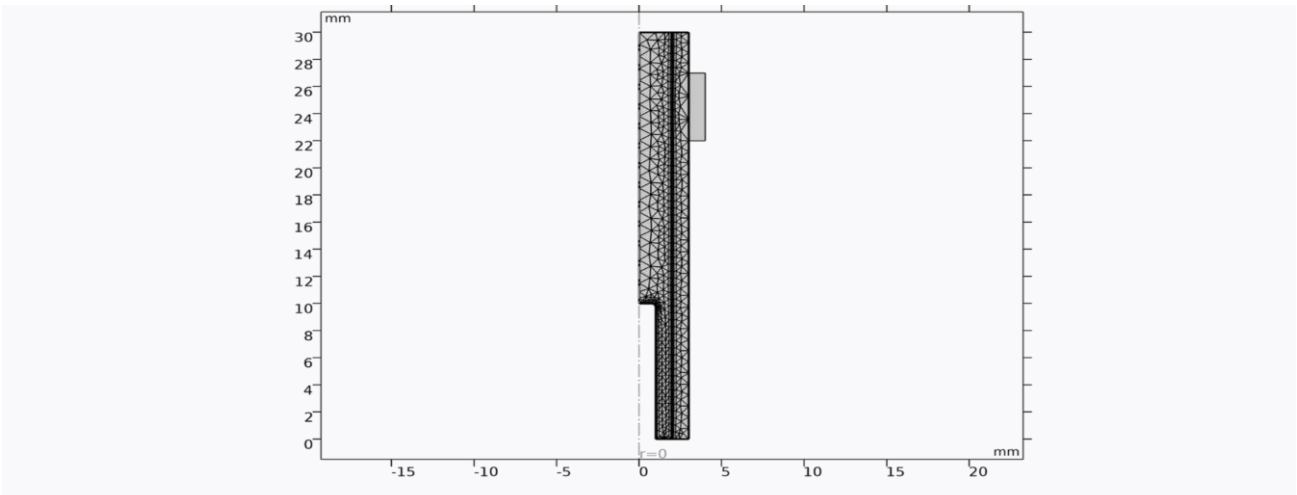


Figure 2. The pin electrode in the atmospheric pressure plasma jet (APPJ) was meshed using the finite element method (FEM).

Results and discussion

Gas flux pattern

Figure 3 shows the gas velocity around the pin electrode for applied voltages of 2 kV and 5 kV. As the applied voltage increases, the maximum velocity increases, whereas the gas velocity decreases as the distance from the pin electrode increases, resulting in electrode cooling. The pin electrode experiences heating because of its high thermal conductivity, which results in the heating of the incoming gas.

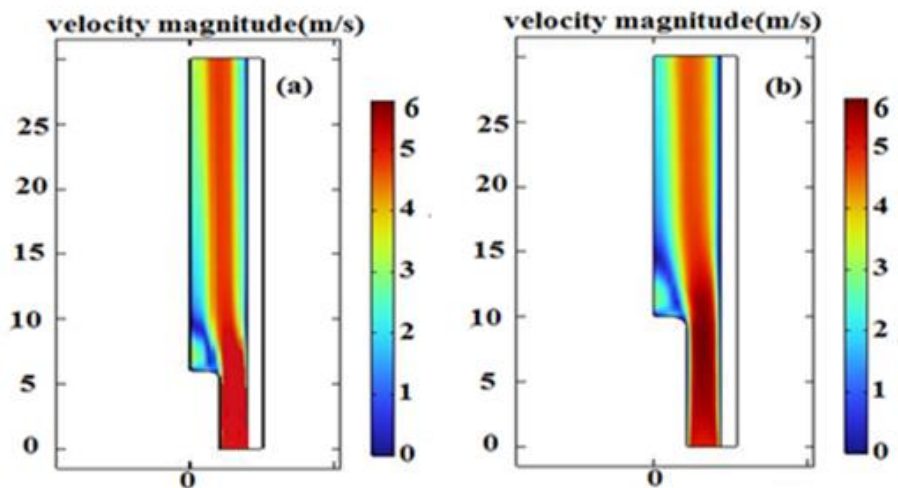


Figure 3. Map of the electron speed distribution for He gas at two different voltages : (a) 2 KV and (b) 5 kV.”

Electron density pattern

We also investigated the evolution of the electron density pattern in the plasma tube. The temporal evolution of the electrical discharge for both 2 kV and 5 kV voltages is shown in Figure 4 and 5, respectively. Initially, the electron density is uniform, but it becomes nonuniform as the discharge

develops. The discharge originates from the edge of the pin electrode, where the electric field is strongest, and creates a plasma region. The discharge is confined around the pin electrode. Subsequently, the plasma region moves along the gas flow direction on the central axis of the plasma jet.

At higher voltages, the electrons detach from the electrode surface and travel toward the outlet of the device with fluid velocity. The electron density reaches 10^{12} (Cm^{-3}) at 2 kV and 10^{13} (Cm^{-3}) at 5 kV. The high electron density around the pin electrode is due to the increased electric field in this region. The density of electrons can increase almost ten times when the voltage increases from 2 kV to 5 kV. This can be attributed to the dependence of the ionization collision cross-section of electrons with helium atoms and increasing the ionization rate with the applied voltage, resulting in a higher electron density. In addition, the electron density at 2 kV is lower than that at 5 kV because the electrons do not have enough energy to cause secondary ionization.

According to Figures 4 and 5, at 5 kV, breakdown appears after 3 μs , and with the passage of time, the density of electrons increases. However, at 2 kV, breakdown appears after about 6 μs , and the electron density is lower than that at 5 kV. This is because higher voltages produce more energetic electrons, which leads to more collisions and a higher ionization rate [23].

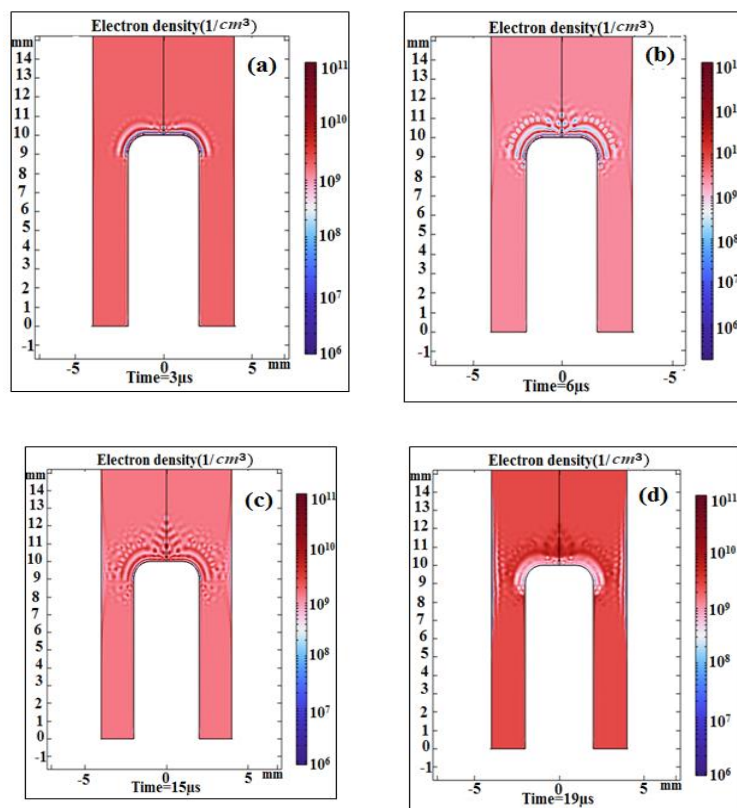


Figure 4. The temporal behavior of the electron density pattern for: (a) 3 μs , (b) 6 μs , (c) 15 μs , and (d) 19 μs for applied voltages of 2 kV.

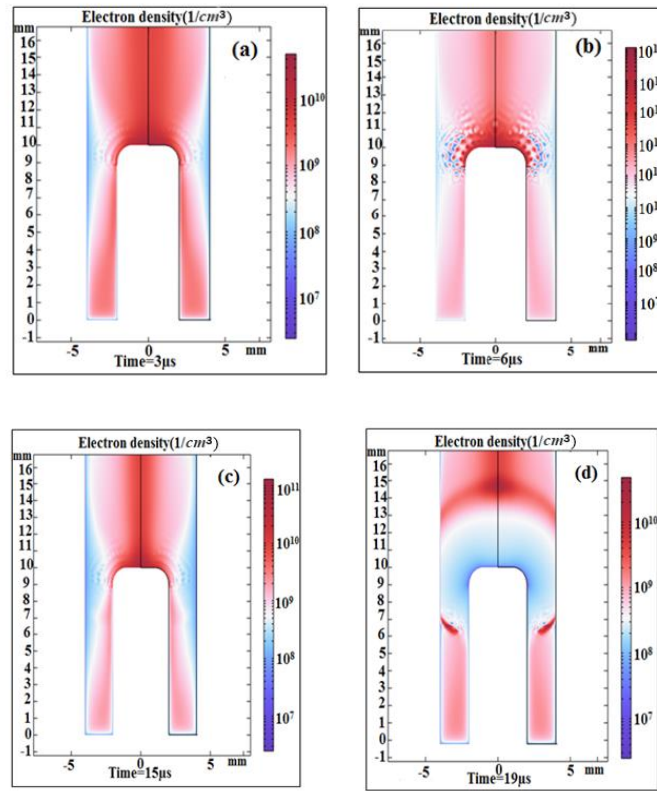
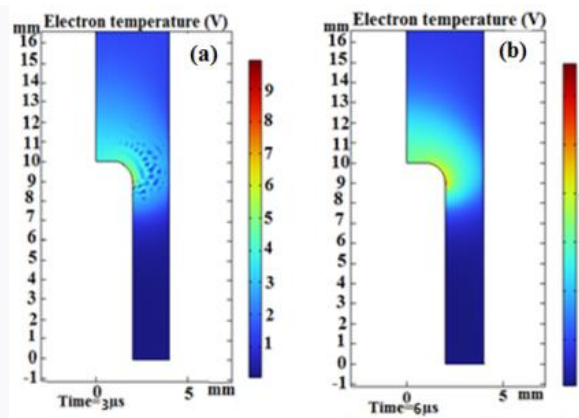


Figure 5. The temporal behavior of the electron density pattern for: (a) 3 μs , (b) 6 μs , (c) 15 μs , and (d) 19 μs for the applied voltages of 5 kV.

The Electron temperature pattern

Since the plasma therapy for cancer cells is one of the applications of plasma jets, it is important to control the plasma temperature to prevent damage to healthy tissue. Plasma jet devices are capable of generating temperatures below 40°C [16]. Figures 6 and 7 illustrate the temperature distribution of electrons for two applied voltages of 2 kV and 5 kV, respectively.



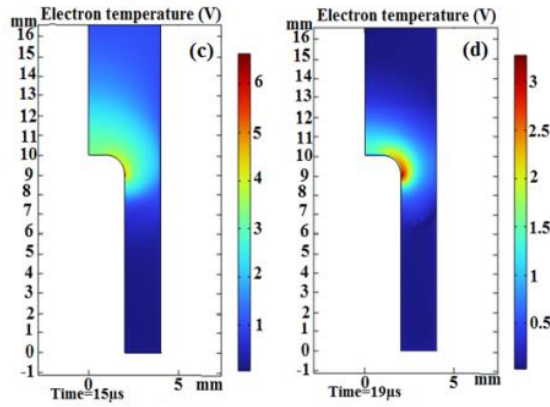


Figure 6: Electron temperature at different times of gas discharge for (a) 3 μs, (b) 6 μs, (c) 15 μs, (d) 19 μs for voltage of 2 kV.

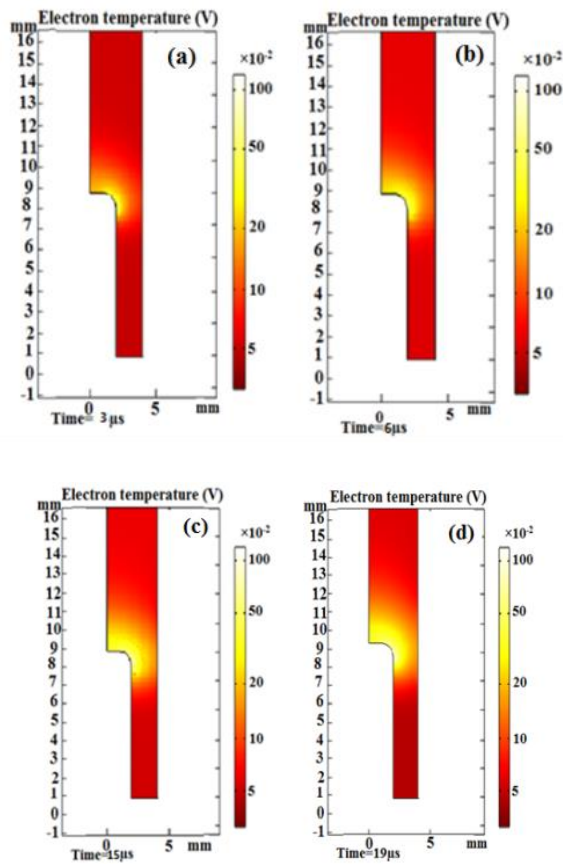


Figure 7. Electron temperature at different times of gas discharge for (a) 3 μs, (b) 6 μs, (c) 15 μs, (d) 19 μs for voltage of 5 kV.

Increasing the applied voltage leads to an increase in the density of electrons within the helium discharge. This is because the higher voltage causes the electrons to gain more energy, resulting in a greater number of collisions and subsequent ionization of the helium atoms. The increased ionization then leads to a higher density of electrons in the discharge [24]. An increase in the

collision of electrons causes more energy exchange between them, which in turn leads to an increase in the electron temperature [25].

An increase in voltage leads to an increase in the density of electrons because it causes electrons to gain more energy, resulting in more collisions and secondary ionization of helium atoms. An increase in the collision of electrons causes more energy exchange between them, which in turn increases the electron temperature.

Figures 6 and 7 illustrate that the temperature profile along the sharp edge of the pin electrode is characterized by higher values, which further increase with the duration of the discharge. The electron temperature is determined by both the average electron energy and electron density, rendering it dependent on the average energy and electron density.

The electron pressure pattern

Figure 8 illustrates the plasma pressure pattern for applied voltages of 2 and 5 kV. The plasma pressure inside the device is not uniformly distributed and increases near sharp edges. Comparison of the pressure pattern inside the device for two different voltages of 2 and 5 kV shows that the applied voltage increases the pressure, which is accompanied by nonuniformity in the pressure pattern. Our findings approximately are in agreement with the results of the results of the Refs. [26-27].

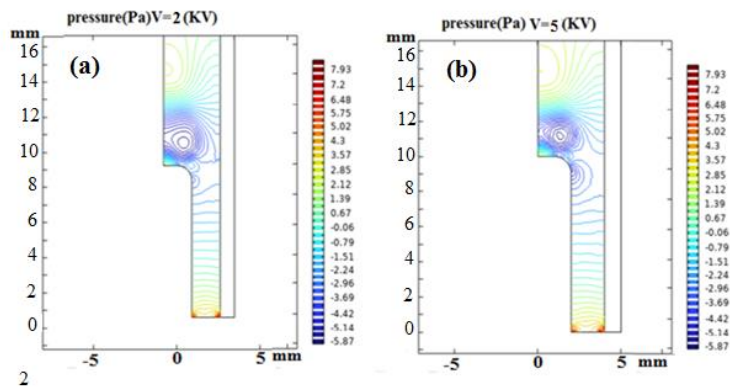


Figure 8. Pattern of plasma pressure inside the plasma tube for voltages of a) 2 kV and b) 5 kV.

The influence of gas working type on plasma jet operation

Figure 9 illustrates the electric potential distribution in the plasma jet device for the working gases of argon and helium. For argon gas, the overall value of the electric potential inside the plasma jet tube is smaller than the helium gas. Therefore, it can be concluded that the average velocity of the ejected helium particles from the plasma jet is higher for helium gas in comparison

to argon gas which are in agreement approximately with the results of the results of the Refs. [28]. However, it is to be noted that for biological application of plasma jet, the kinetic energy of the plasma species has the key role.

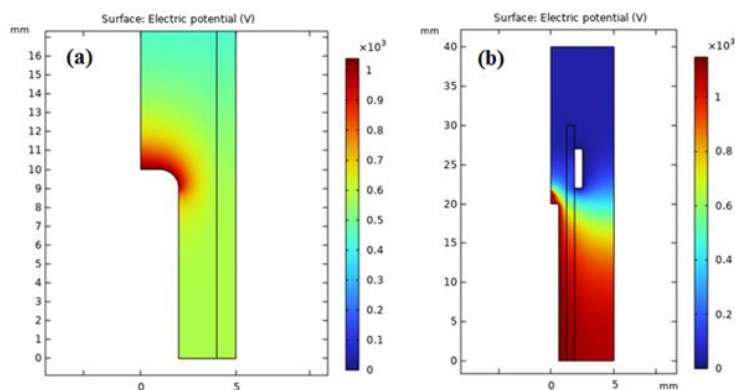


Figure 9. The electric potential distribution inside the plasma jet device for voltage of 2 kV, time = 9 μ s for a) Helium and b) Argon.

Conclusion

In this study, we investigated the changes in effective plasma parameters to treatment, such as electron density and temperature, through the 2D COMSOL simulation for two applied voltage values. It was observed that as the voltage increased, both the electron density and electron temperature increased. At an input voltage of 5 kV, the maximum electron density was approximately 10^{15} Cm^{-3} and the maximum electron temperature was approximately 5 eV. For a lower applied voltage of 2 kV, the electron density was approximately 10^{12} Cm^{-3} and the maximum electron temperature was approximately 5 eV. To examine the changes in speed, it was observed that at an input voltage of 5 kV, the maximum gas velocity was approximately 6 m/s, whereas at an input voltage of 2 kV, the maximum gas velocity was approximately 5 m/s. Additionally, it was observed that as the input voltage increased, the plasma pressure and its nonuniformity inside the plasma tube also increased.

These values indicated that the plasma operated within the bright discharge region without the occurrence of electric arcs, making it suitable for biomedical applications. However, it is worth mentioning that at discharge voltages exceeding 5KV, the temperature rose due to the increased presence of energetic electrons and an electric arc was created. In addition, using the gases with the smaller mass resulted to the increasing the electric potential inside the plasma jet device.

Reference

1. Min T, Xie X, Ren K, Sun T, Wang H, Dang C, Zhang H. Therapeutic Effects of Cold Atmospheric Plasma on Solid Tumors. *Frontiers in Medicine*. 2022;9(13):1.
2. Yan D, Sherman JH, Keidar M. Cold atmospheric plasma, a novel promising anti-cancer treatment modality. *Oncotarget*. 2017;8(9):15977-15995.
3. Murillo D, Huergo C, Gallego B, Rodríguez R, Tornín J. Exploring the Use of Cold Atmospheric Plasma to Overcome Drug Resistance in Cancer. *Biomedicines*. 2023;11(1):208
4. Yan D, Xu W, Yao X, Lin L, Sherman JH, Keidar M. The Cell Activation Phenomena in the Cold Atmospheric Plasma Cancer Treatment. *Scientific Reports*. 2018;8(1):15418. doi: 10.1038/s41598-018-29740-2.
5. Živanić M, Espona-Noguera A, Lin A, Canal C. Current State of Cold Atmospheric Plasma and Cancer-Immunity Cycle: Therapeutic Relevance and Overcoming Clinical Limitations Using Hydrogels. *Advanced Science (Weinh)*. 2023;10(8):e2205803.
6. Pipa AV, Reuter S, Foest R, Weltmann KD. Controlling NO Production of an Atmospheric Pressure Plasma Jet. *Journal of Physics D: Applied Physics*. 2012;45(8):085201.
7. Park J, Henins I, Herrmann HW, Selwyn GS, Hicks RF. Discharge phenomena of an atmospheric pressure radio-frequency capacitive plasma source. *Journal of Applied Physics*. 2001;89(1):20-28.
8. Lieberman MA, Lichtenberg AJ. *Principles of Plasma Discharges and Materials Processing*. John Wiley & Sons; 2005 Apr 8.
9. Laroussi M. Cold Plasma in Medicine and Healthcare. *The New Frontier in Low Temperature Plasma Applications*. *Frontiers in Physics*. 2020;8:528206.
10. Lu X, Naidis G, Laroussi M, Reuter S, Graves DB, Ostrikov K. Reactive Species in Non-Equilibrium Atmospheric-Pressure Plasmas: Generation, Transport, and Biological Effects. *Physics Reports*. 2016;630(4):1-84.
11. Bashkani ET, Yasserian K, Hosseini HM, Borghei M, Sari AH. Optimization of atmospheric low temperature plasma to reduce side effects in colorectal cancer. *Brazilian Journal of Physics*. 2022;52:181.
12. Torabibashkani E, Yasserian K, Mahmoodzadeh H, Borghei M, Sari A. Optimization of Atmospheric Low-Temperature Plasma to Reduce Side Effects in Colorectal Cancer.
13. Hadefti A, Leprovots M, Thulliez M, et al. Cold atmospheric plasma differentially affects cell renewal and differentiation of stem cells and APC-deficient-derived tumor cells in intestinal organoids. *Cell Death Discovery*. 2022;8(1):66.

14. Amiri Y, Ghasemi B, Shahbazi Rad Z. Two-dimensional modeling of atmospheric-pressure cold plasma jet generator for treatment application. *Radiation Physics and Chemistry*.2022; 188:109462
15. Lin P, Zhang J, Nguyen T, Donnelly VM. Numerical simulation of an atmospheric pressure plasma jet with coaxial shielding gas. *Journal of Applied Physics*. 2021;129(5):075205.
16. Schweigert I, Zakrevsky DE, Milakhina E, Gugin PP. Low temperature plasma jet optimization for cancer treatment. In: 16th International Conference on Modification of Materials with Particle Beams and Plasma Flows Beam and Plasma Sources, 2022. p. 212.
17. Tavant A, Croes V, Lucken R, Lafleur T, Bourdon A, Chabert P. The effects of secondary electron emission on plasma sheath characteristics and electron transport in an $E \times B$ discharge via kinetic simulations. *Plasma Sources Science and Technology*. 2018; 27: 124001.
18. Moribayashi K. Effect of Coulomb interaction between secondary electrons on plasma formation due to heavy-ion irradiation. *Journal of Physics*. 2022;27(8):083701.
19. Hershkowitz N, Goettsch RL, Chan C, Hendricks K. Detection of secondary electrons in a multidipole plasma. *Journal of Physics*. 1982;53(10):5330-5332.
20. Hagela GJM, Pitchford LC. Solving the Boltzmann equation to obtain electron transport coefficients and rate coefficients for fluid models. *Plasma Sources Science and Technology*. 2005;14(4):722.
21. Golubovskii YuB, Maiorov VA, Behnke J, Behnke JF. Influence of interaction between charged particles and dielectric surface over a homogeneous barrier discharge in nitrogen. *Journal of Physics D: Applied Physics*. 2002;36(3):751.
22. Pal U, Sharma AK, Soni JS, Kr S, Khatun H, Kumar M, Meena BL, Tyagi MS, Lee BJ, Iberler M. Electrical modelling approach for discharge analysis of a coaxial DBD tube filled with argon. *Journal of Physics D: Applied Physics*.2009;42(4):045213.
23. Deepak GD, Joshi N, Prakash R. Model analysis and electrical characterization of atmospheric pressure cold plasma jet in pin electrode configuration. *AIP Advances*. 2018;8(5):055321.
24. Zaihao L, Yinghua L, Shuang R, Boping X, Peiqi Y, Jing L, Yishan W, Wei Z, Hui W, Jie T. Numerical simulation of the large-gap and small-gap pre-ionized direct-current glow discharges in atmospheric helium, *Physics of Plasmas*. 2023; 30: 043507.
25. Weltmann KD, Kindel E, Woedtke T. Atmospheric-pressure plasma sources: Prospective tools for plasma medicine. *Pure and Applied Chemistry*. 2010;82(6):1223-1237.

26. Goel V, R. Kar, Roy A, Patil D. S, Maiti N, Optimization of Spatial Parameters of a 2.45-GHz Atmospheric Pressure Cold Plasma Jet: Comparison Between Multiphysics Simulation and Experimental Results, *IEEE Transactions on Plasma Science*. 2022; 50(10): 3539-3546.
27. Liu X, Zhang J, Luo C, Dang M, Lin M, Zhang P. Experiment and simulation of electron density distribution in discharge plasma at hypersonic speed. *AIP Advances* (2023); 13: 095307.
28. Vichiansan N, Leksakul K, Chaopaisarn P, Boonyawan D. Simulation of simple 2D plasma jet model for NO, OH, and H₂O₂ production via Multiphysics in laminar flow and transport of diluted species through design of experiment method.” *AIP Advances* 11 (2021); 25: 035040.